

ELECTRONIC SUPPLEMENTARY INFORMATION

Large area inkjet-printed metal halide perovskite LEDs ened by gas flow-assisted drying and crystallization

Vincent R. F. Schröder,^a Nicolas Fratzscher,^b Felix Hermerschmidt,^b Florian Mathies,^c
Edgar Nandayapa,^a Eva L. Unger^{c,d,e} and Emil J. W. List-Kratochvil^{*a,b}

- a. Helmholtz-Zentrum Berlin für Materialien und Energie GmbH, Hahn-Meitner-Platz 1, 140109 Berlin, Germany
- b. Institut für Physik, Institut für Chemie, Humboldt-Universität zu Berlin, IRIS Adlershof, Zum Großen Windkanal 2, 12489 Berlin, Germany
- c. Department Solution Processing of Hybrid Materials & Devices, Helmholtz-Zentrum Berlin für Materialien und Energie, Kekuléstraße 5, 12489 Berlin, Germany
- d. Hybrid Materials: Formation and Scaling, IRIS Adlershof, Humboldt Universität zu Berlin, Am Großen Windkanal 2, 12489 Berlin, Germany
- e. Chemical Physics and NanoLund, Lund University, PO Box 124, 22100 Lund, Sweden

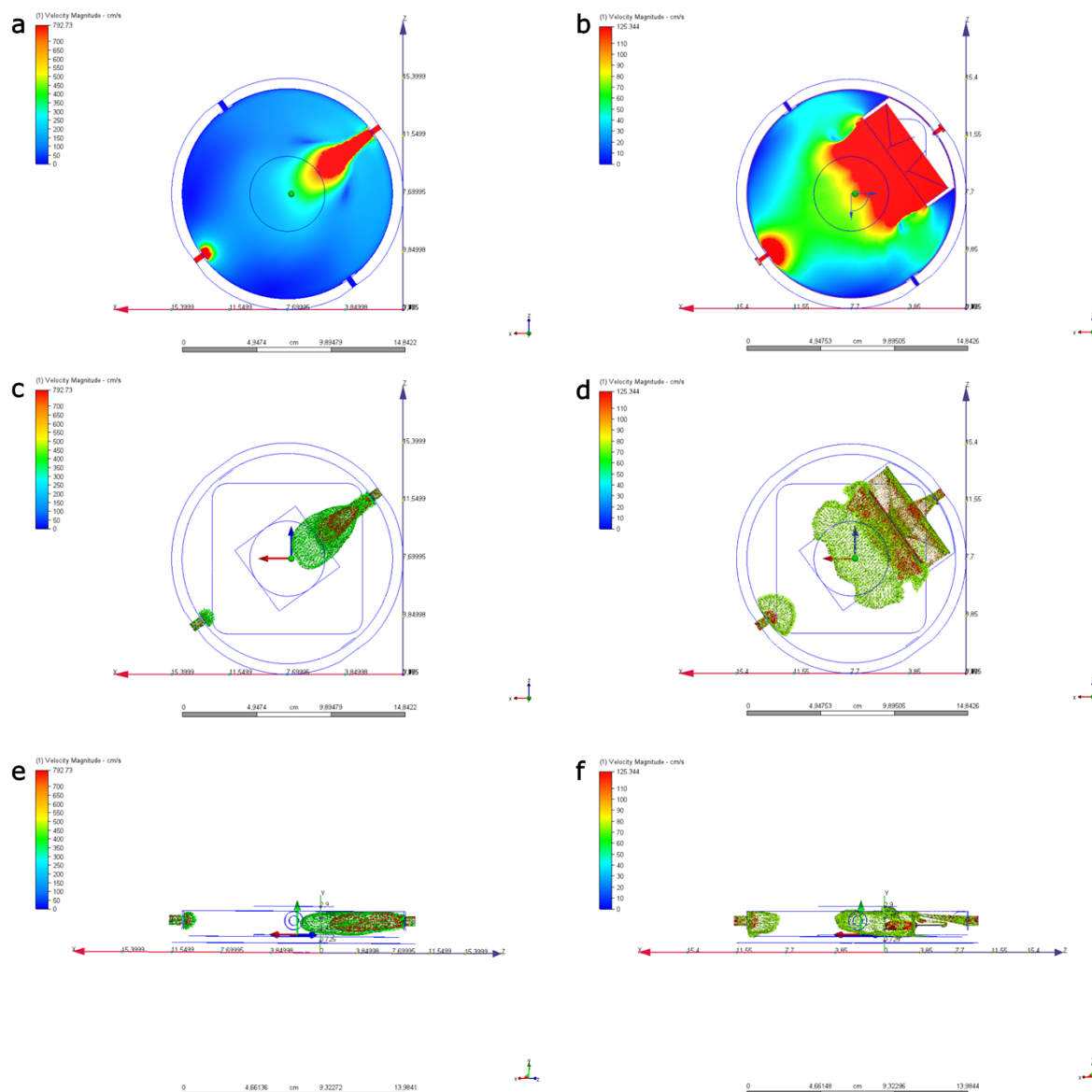


Figure S1: Gas flow simulations of the incoming nitrogen flow in the evacuated gas flow assisted drying (GAVD) chamber. The utilized slit nozzle softens and broadens the nitrogen flow, which can be seen in the distribution of the flow velocity magnitude (a,b) as well as the velocity vectors in (c,d) top and (e,f) side view.

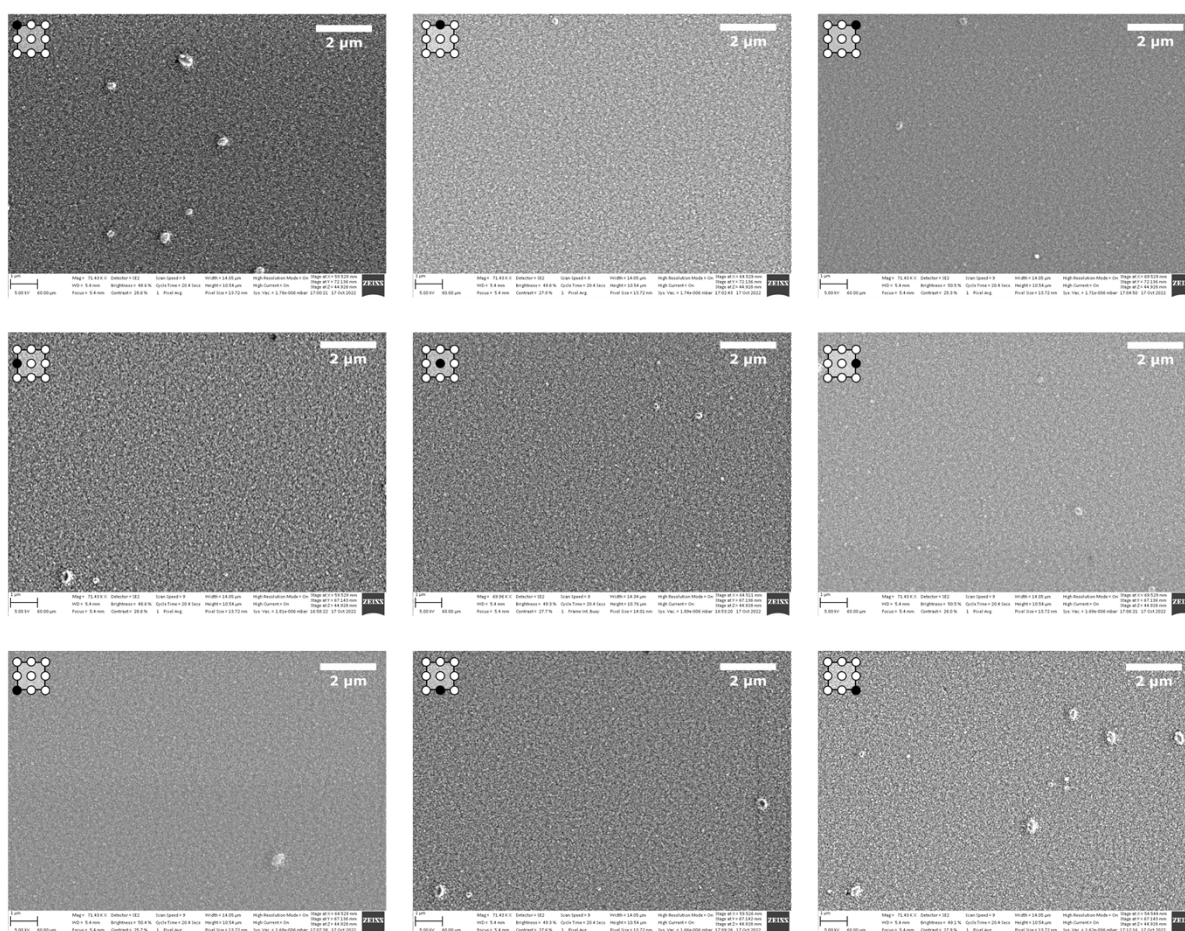


Figure S2: Scanning electron microscope images of inkjet-printed perovskite layers. In a $10 \times 10 \text{ mm}^2$ square, SEM images were taken in the corners, on the edges and in the centre to demonstrate uniformity over a large area.

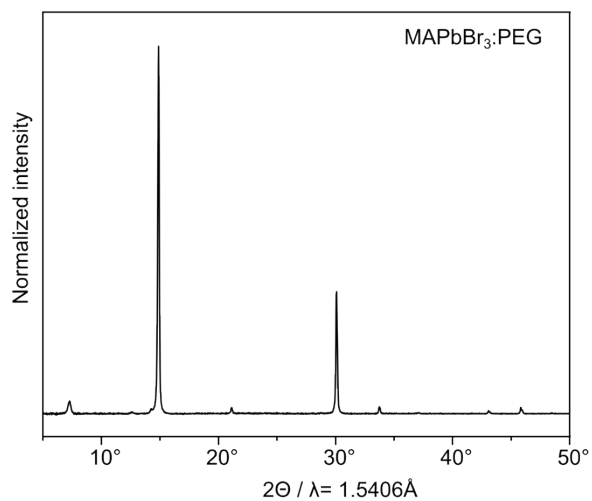


Figure S3: XRD of the inkjet-printed perovskite layers. Recorded in Bragg-Brentano geometry and equivalent to previously obtained diffraction pattern.¹⁴

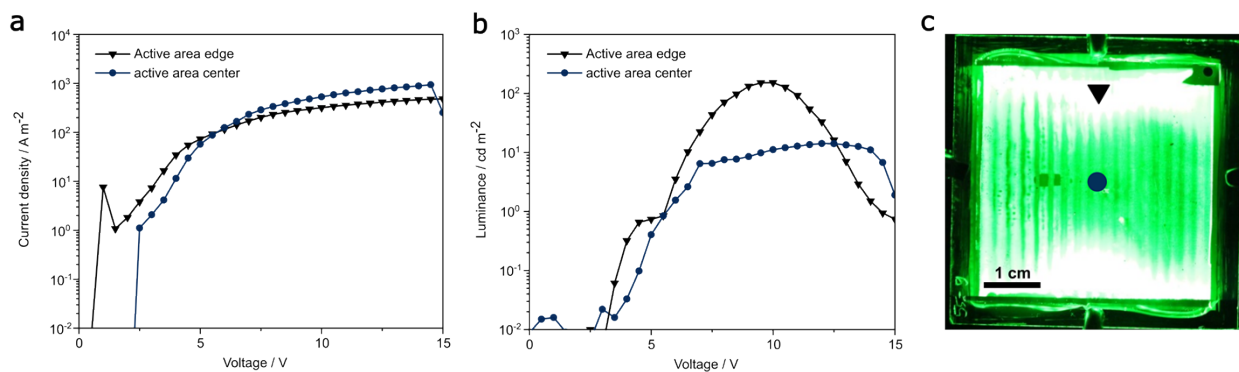


Figure S4: (a) Current-voltage and (b) luminance-voltage characteristics of 1600 mm² PeLED devices with 20 nm BCP contact layer. The luminance was measured at the edge of the device, near the contact to the ITO electrode, and in the centre of the device. (c) The positions of the measurements are indicated in the photo.

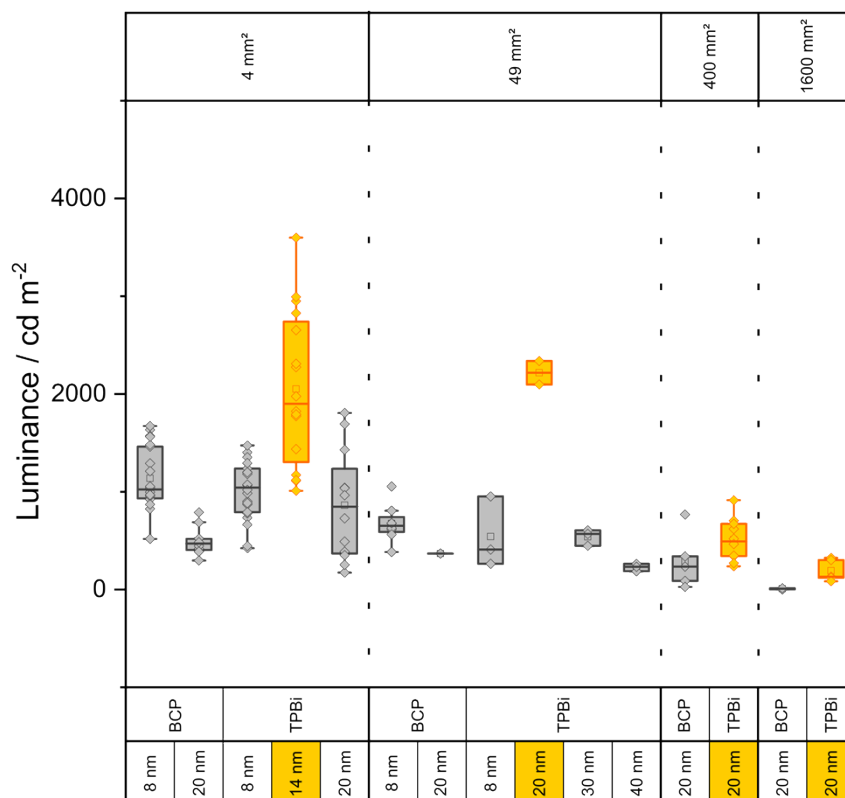
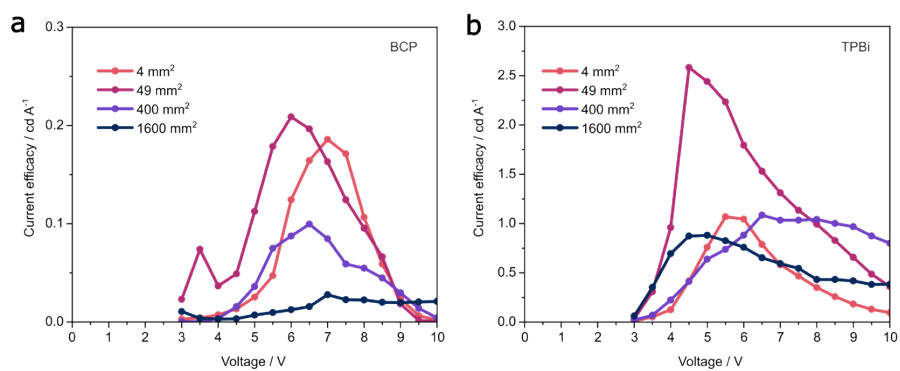


Figure S5: Luminance distribution for fabricated PeLED devices depending on active area size, contact layer material and contact layer thickness, whereby devices containing TPBi consistently yield higher luminance values than devices containing BCP.



Figur

e S6: Current efficacy characteristics of PeLEDs using (a) BCP and (b) TPBi as contact layers.

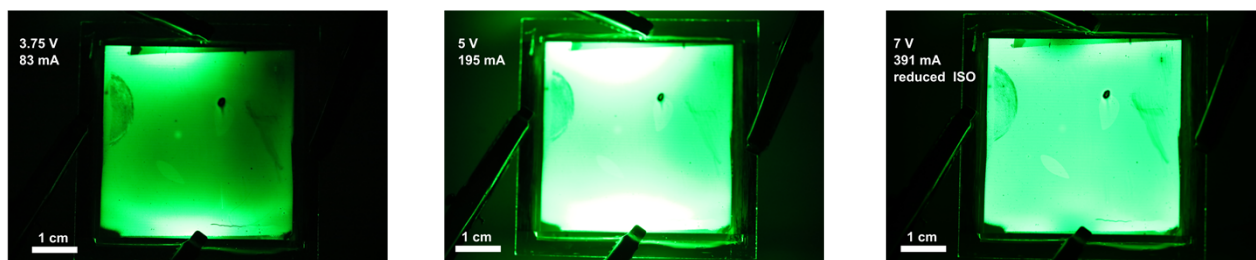


Figure S7: Photo of a 1600 mm² TPBi-containing PeLED showing inhomogeneous emission due to high series resistance at lower voltages and reduction of the luminance gradient with increasing voltage.